ISSN 0208-7774 TRIBOLOGIA 3/2023 p. 19–29
DOI: 10.5604/01.3001.0053.9426

Mateusz DZIUBEK[*], Małgorzata RUTKOWSKA-GORCZYCA[**], Dominika GRYGIER[***]

THE EFFECT OF THE AUSTENITISATION TEMPERATURE FOR THE TWO-STAGE HEAT TREATMENT OF HIGH-MANGANESE STEELS ON ITS WEAR RESISTANCE UNDER ABRASIVE CONDITIONS

WPŁYW TEMPERATURY PRZESYCANIA W DWUSTOPNIOWEJ OBRÓBCE CIEPLNEJ STALI WYSOKOMANGANOWEJ NA ODPORNOŚĆ NA ZUŻYCIE ŚCIERNE

Key words: high manganese steel, abrasive wear, microstructure, hardness, heat treatment.

Abstract: Fine-grained high-manganese X120Mn12 grade steel was subjected to a two-stage heat treatment consisting of long-term isothermal annealing at 510°C, which was followed by resaturation in order to reduce the negative effect of the brittle carbide carbides of manganese cementite $(Fe,Mn)_3C$. The objective of the experiment was to elucidate the effects of distinct stages of heat treatment on the properties of high manganese steel with regard to its resistance to abrasive wear. Supersaturation was performed for eleven different variations of temperature values ranging from 600°C to 1100°C to verify its effect on the resistance to abrasion wear under abrasion conditions. An increase in the supersaturation temperature results in the gradual coagulation and disintegration of the colonies of pearlite and needle-like carbides $(Fe,Mn)_3C$ formed during isothermal annealing. At the same time, as a result of the PSN (particle stimulated nucleation) process, the microstructure of austenite undergoes partial refinement, which ultimately increases the resistance to abrasive wear. As a result of the final microstructural changes resulted in an increase in the resistance to abrasion of approximately 6% compared to the initial state.

Słowa kluczowe: stal wysokomanganowa, zużycie ścierne, mikrostruktura, twardość, obróbka cieplna.

Streszczenie: Drobnoziarnistą stal wysokomanganową gatunku X120Mn12 poddano dwustopniowej obróbce cieplnej złożonej z długoterminowego izotermicznego wygrzewania w temperaturze 510°C, a następnie ponownemu przesycaniu w celu zredukowania negatywnego wpływu kruchych wydzieleń węglików cementytu manganowego $(Fe,Mn)_3C$. Eksperyment miał na celu poznanie wpływu poszczególnych etapów obróbki cieplnej na właściwości stali wysokomanganowej w kontekście odporności na zużycie ścierne. Etap przesycania zrealizowano dla jedenastu różnych wariantów wartości temperatury z zakresu od 600°C do 1100°C w celu zweryfikowania jej wpływu na odporność na zużycie ścierne. Wzrost temperatury przesycania skutkuje stopniową koagulacją oraz rozpadem powstałych w trakcie wyżarzania izotermicznego kolonii perlitu oraz iglastych węglików $(Fe,Mn)_3C$. Jednocześnie w wyniku procesu PSN (ang. *particles stimulated nucleation*) mikrostruktura austenitu ulega częściowemu rozdrobnieniu, co finalnie wpływa na wzrost odporności na zużycie ścierne. W wyniku końcowych zmian mikrostrukturalnych uzyskano wzrost odporności na ścieranie o około 6% w porównaniu do stanu wyjściowego dla wariantu obróbki cieplnej złożonego z etapu długoterminowego izotermicznego wyżarzania w temperaturze 510°C oraz następującego po nim przesycania w temperaturze 750°C. Wzrost odporności wywołany został wydzieleniem globularnych węglików $(Fe,Mn)_3C$ oraz powstaniem nowych ziaren austenitu.

[*] ORCID: 0000-0002-6179-9771. Wroclaw University of Science and Technology, Faculty of Mechanical Engineering, Department of Vehicle Engineering, Wybrzeże Wyspiańskiego 27, 50-370 Wrocław, Poland, e-mail: mateusz.dziubek@pwr.edu.pl.

[**] ORCID: 0000-0003-2712-5914. Wroclaw University of Science and Technology, Faculty of Mechanical Engineering, Department of Vehicle Engineering, Wybrzeże Wyspiańskiego 27, 50-370 Wrocław, Poland, e-mail: malgorzata.rutkowska-gorczyca@pwr.edu.pl.

[***] ORCID: 0000-0001-7062-6357. Wroclaw University of Science and Technology, Faculty of Mechanical Engineering, Department of Vehicle Engineering, Wybrzeże Wyspiańskiego 27, 50-370 Wrocław, Poland, e-mail: dominika.grygier@pwr.edu.pl.

INTRODUCTION

High manganese steel is utilised for components exposed to impact or high unit pressure loads. Its most prominent characteristic is the ability to undergo self-strengthening under high dynamic stresses under natural operating conditions. This strengthening results from the twinning mechanism and strain hardening that generate dense dislocation structures **[L. 1**, **2]**. Consequently, a high-hardness surface layer is formed, and the steel retains the plasticity of the unhardened core, enabling its application in various industrial fields, including open-pit mining **[L. 3]**. However, inadequate working stresses do not guarantee steel hardening and may significantly reduce its service life due to low resistance to abrasive wear. In this context, it is crucial to understand the wear mechanisms, where the friction pair consists of two solid bodies and a third body comprising of dust and/or loose particles. The third body can move over the surface of the element, in turn grinding it or damaging the surface layer by impact **[L. 4]**. The relatively high contribution of abrasive interaction represents a challenge to improving the resistance of high manganese steel to abrasive wear.

These experiments are primarily conducted by modifying the chemical composition of high manganese steels, often achieved through alloying with carbide-forming or grain-refining elements **[L. 5–11]**. The intended outcome of these material modifications is to have an equivalent effect on assessing the wear resistance of high manganese steel, as well as the duration and character of the load. The selection of the material morphology must correspond to the working conditions of the element **[L. 12]**.

Another direction of development involves the development of high manganese steel heat treatment, which allows an increase in wear resistance. The selection of heat treatment parameters is crucial in shaping the material's microstructure and, consequently, the mechanical properties of the steel. One of these parameters is the selection of the austenitisation temperature, which not only increases tensile strength but also decreases plasticity, elongation, impact toughness, and hardness as temperature increases, which is directly related to the growth of the grain size of the austenite **[L. 13]**. The cooling rate from the supersaturation temperature also has a significant impact, with an increase in the cooling rate-limiting the amount of precipitated carbides. The results of mechanical tests have shown that quenching high manganese steel in a salt bath decreases plasticity, tensile strength, and hardness while increasing impact toughness **[L. 14]**.

Additionally, research teams are conducting experiments based on modifying the processing parameters and the number and type of heat treatments. Double austenitisation **[L. 15]** or two-step heat treatment consisting of long-term isothermal annealing at 260°C to 550°C and reaustenitisation is performed. Isothermal annealing leads to the precipitation of numerous colonies of fine-grained pearlite and M3C-type carbides, which undergo reconstruction during supersaturation in the second stage, in turn resulting in steel recrystallisation. This improves mechanical properties compared to steels produced by the one-stage austenitising annealing method **[L. 16**–**18]**.

The occurring process of recrystallisation during the two-step heat treatment of high-manganese steel exhibits the particle stimulated nucleation mechanism (PSN), which was observed by Humphrey in aluminium alloys **[L. 19–22]**.

Modifying the heat treatment and/or chemical composition of steel results in changes in the morphology of the microstructure, with the construction, homogeneity, and multiphase nature affecting the changes in the material's wear resistance. Steels with a similar hardness but different microstructure morphology can significantly differ in the degree of abrasive wear **[L. 4]**. Moreover, the influence of the character of precipitates and the precipitates' shape and distribution on wear resistance is an area of research for many researchers. **[L. 23**–**28]**.

Finally, the interaction between particles and the surface has a different character, classified through material removal mechanisms or stress interaction modes **[L. 29, 30]**. In the case of high manganese steel, the most common wear mechanisms are microcutting and microploughing **[L. 31]**.

OBJECT AND METHODOLOGY OF THE STUDY

This study used a commercially available fine-grained high-manganese X120Mn12 grade steel as the research material. The study aimed to analyse changes in the wear resistance of high-manganese steel subjected to various heat treatment variants

consisting of two stages. The first stage involved the isothermal annealing of samples in a protective atmosphere of 99.99% argon for 6 hours at a temperature of 510°C, followed by furnace cooling. The second stage involved reaustenitisation of the samples in a temperature range of 600°C – 1100°C with a step of 50°C, heating them for 5 minutes, and then cooling them with water. The scheme of the implemented experiment is presented in **Fig. 1**.

In the isothermally annealed state, the microstructure of high manganese steel consists of an austenitic matrix, $(Fe,Mn)_3C$ carbides located at the grain boundaries of the former austenite in the form of a continuous network, needle-like $(Fe,Mn)_3C$ carbide precipitates, and colonies of fine-grained pearlite. After reaustenitising coarse-grained steel at 900°C, the material showed a 16.4% increase in wear resistance under abrasion

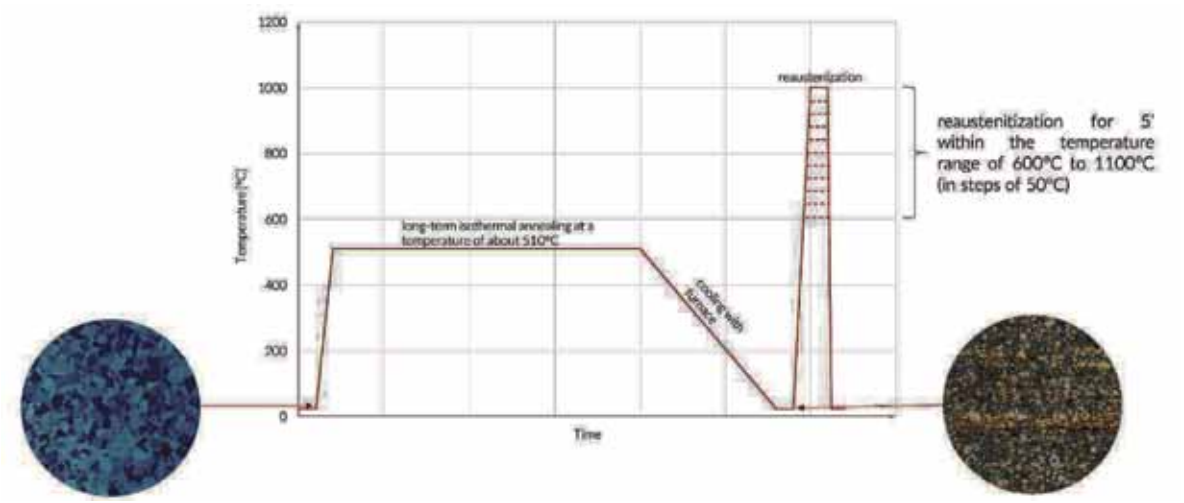

Fig. 1. Schematic representation of the performed experiment
Rys. 1. Schematyczna reprezentacja wykonanego eksperymentu

conditions **[L. 32]**. In the present study, a similar research hypothesis regarding the effect of two-stage heat treatment on the wear resistance of X120Mn12 steel, which in this case, has a fine-grained structure, was verified.

The chemical composition of the starting material was determined by optical emission spectroscopy using a Leco GDS-500A spark emission analyser. A series of replicates on the ground surface of the analysed material were carried out in extremely localised areas of the sheet to confirm the homogeneity of the chemical composition of the material intended for the experiment and exclude any possible decarburisation of the steel.

The heat treatments of the steel samples were carried out using a laboratory FCF22SH muffle furnace from Czylok. Each sample was subjected to observations using optical microscopy, scanning electron microscopy, and hardness measurements.

Observations of the morphology of the microstructure in the etched state with 5% nitric acid were made using a Nikon Eclipse MA 200 metallographic light microscope equipped with a Nikon DS-Fi5 CCD camera and a Phenom XL scanning electron microscope. SEM observations of the surface subjected to abrasive wear tests were carried out using topographic contrast (SE detector) and material contrast (BSE detector) at an accelerating voltage of 15 kV.

Hardness measurements were carried out using the Vickers method according to the PN-EN ISO 6507-1:2018-5 standard. Measurements with a load of 294.2 N (HV30) were performed using the Zwick/Roell ZHU 187.5 hardness tester.

A wear resistance test was performed for each material state using a T-07 type tribotester. The test was carried out according to the GOST 23.208-79 standard, where a constant load with a force of F = 44.0 ±0.25 N was applied, and corundum particles with a grain size of 90 were used as the abrasive material according to the ISO 8486-2:2007 standard. For each variant of the material state, three repetitions were carried out, with a test

lasting 10 minutes being performed (600 cycles). The relative wear resistance coefficient Kb was calculated in accordance with GOST 23.208-79, where X120Mn12 steel in the as-received state was used as the reference material. The obtained results were analysed using the Statistica 13 program (Student's t-test for $p < 0.01$ and $\alpha = 0.05$).

RESULTS AND DISCUSSION

The microstructure morphology was evaluated for each obtained state of the X120Mn12 steel. Microscopic images were compiled on the same scale in the form of a graphical presentation, with the mechanisms occurring during the temperature rise of reaustenisation indicated (**Fig. 2**).

In the as-delivery state, the tested material is characterised by fine-grained, homogeneous austenite with visible characteristic twin boundaries. The grain size corresponds to the value of the parameter G = 10.0 (A = 127.161 μm^2) according to the ASTM E112-13 standard. This is a typical morphology for oversaturated and recrystallised Hadfield steel after plastic deformation, resulting in a typical form of austenite with straight and twin grain boundaries. The steels also lack carbide precipitates that could create a continuous network along the grain boundaries, significantly degrading the material's quality. The observed material lacks grain size, non-uniformities, a dendritic structure, cracks, or porosity across its cross-section.

After the isothermal annealing process, a significantly refined microstructure was obtained compared to the delivered state. The microstructure consisted of carbide $(Fe,Mn)_3C$ precipitates, numerous colonies of fine-grained pearlite, and an austenitic matrix. The carbides $(Fe,Mn)_3C$ take on a dual form: a continuous coating along the boundaries of the former austenite inherited from the delivered state and needle-like precipitates. A similar microstructure morphology was obtained during studies carried out for coarse-grained X120Mn12 steel **[L. 32]**.

In the temperature range of 600°C to 850°C, $(Fe,Mn)_3C$ carbides, both in the form of needles and those forming the fine-grained pearlite of individual

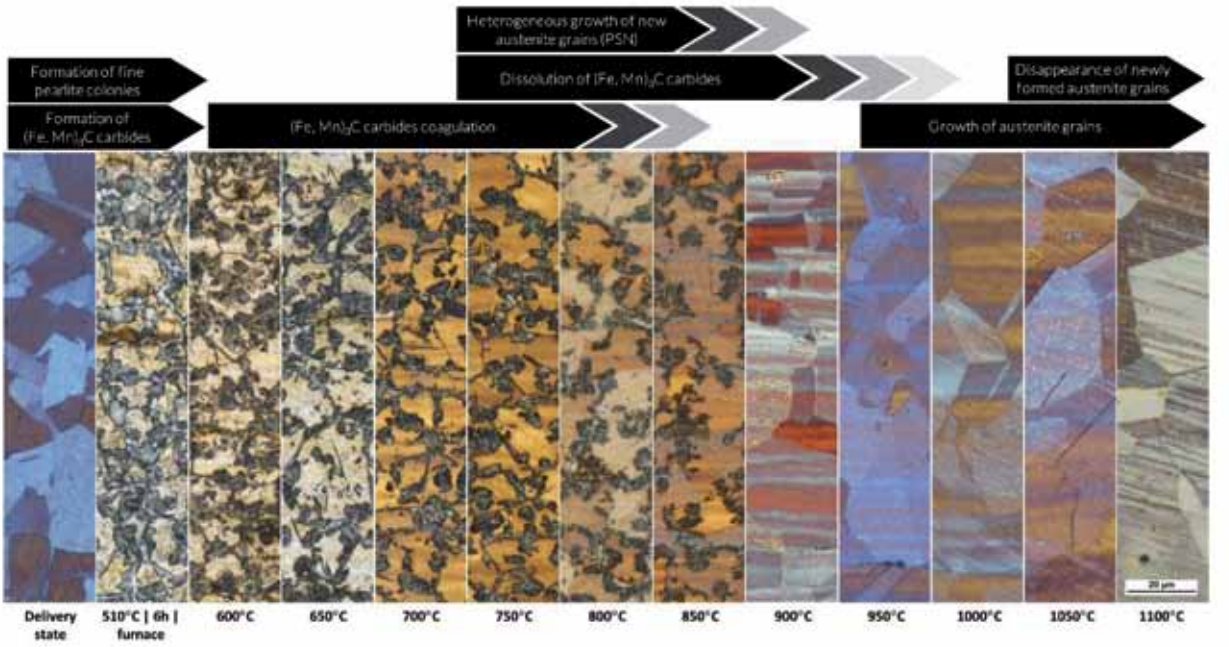

Fig. 2. Graphical representation of the morphological changes and processes that occur with the increasing reaustenitising temperature. Summary of the morphology of the microstructure for different states of X120Mn12 steel: the delivery state, the state after isothermal annealing, and the states after different temperature variants of resaustenisation (600°C – 1100°C). Etched state

Rys. 2. Graficzna reprezentacja zmian morfologicznych oraz procesów zachodzących wraz ze wzrostem temperatury ponownego przesycania. Zestawienie morfologii mikrostruktury dla różnych stanów stali X120Mn12: stanu dostarczenia, stanu po izotermicznym wygrzewaniu oraz stanów po różnych wariantach temperaturowych reaustenityzacji (600°C – 1100°C). Stan trawiony

colonies, underwent a process of coagulation, in turn causing changes in the morphology of the microstructure.

Furthermore, above 750°C, the M3C-type carbides and fine-grained pearlite colonies gradually disappeared during isothermal annealing until homogeneous austenite was obtained at temperatures between 900°C and 950°C. Additionally, for the 900°C variant, individual new austenite grains (with a size smaller than 20 μm) with characteristic twin boundaries were visible both inside the primary austenite grains and at their boundaries (**Fig. 3**). Their presence is a result of the PSN mechanism. M3C carbides and fine-grained pearlite colonies were heterogeneous nucleation sites, forming new grains. However, the simultaneous growth of primary austenite grains was also visible, which increased the average grain size to the value of parameter G = 9.5 (A = 167,299 μm^2).

The return to the original microstructure occurs at around 1000°C, when all the changes obtained due to the two-stage heat treatment disappear, causing the obtained microstructure to have a form similar to the delivered state. Above this temperature, the disappearance of newly formed grains is observed, and there is a significant increase in the size of the austenite grain to the value of G = 5.0 (A = 3456.702 μm^2).

The processes occurring during reaustenitisation result in a decrease in hardness values with an increase in saturation temperature (**Fig. 4**). A sudden drop in hardness occurred at the lowest saturation temperatures, i.e., 600°C – 700°C, which is due to the coagulation of the needle-like M3C carbides and manganese cementite contained in the colonies of the fine-grained pearlite. In subsequent stages, the decrease in hardness occurred more gradually, which is related to the gradual dissolution of the carbides precipitated during isothermal annealing. This decrease can be compensated to some extent by strengthening the boundaries of newly-formed grains due to the PSN mechanism. Above the temperature of 900°C, the hardness of the material stabilised, with the emerging drop in this value being related to the growth of the austenite grain.

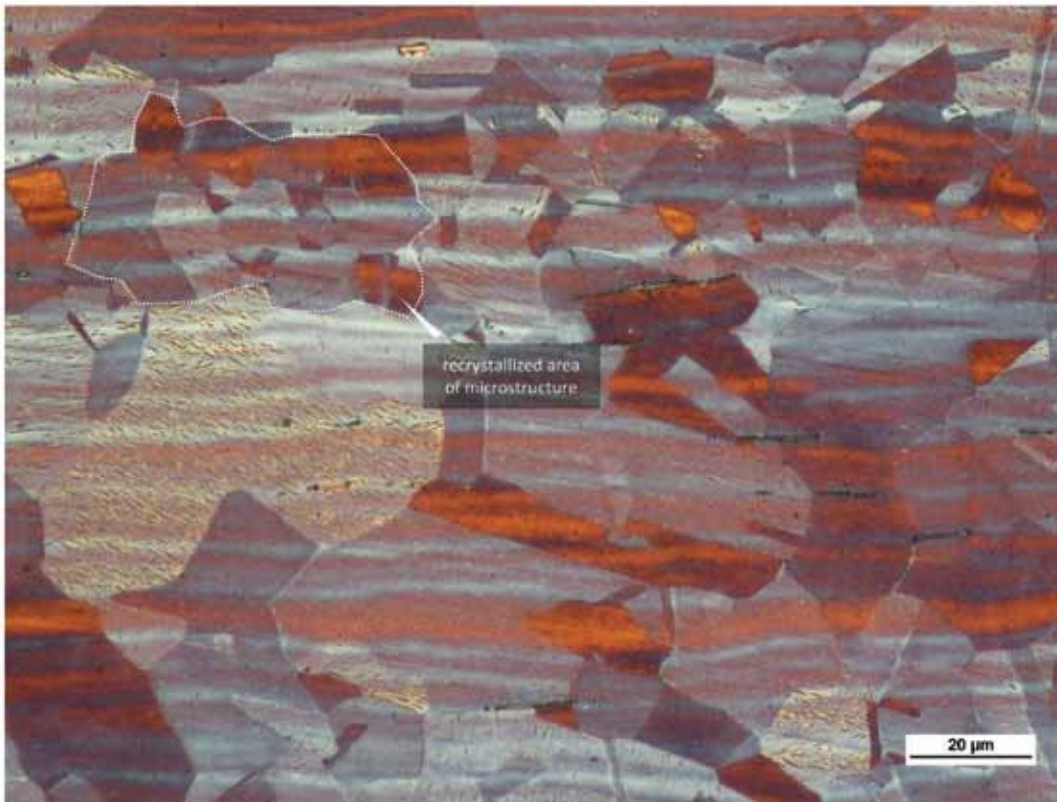

Fig. 3. Microstructure of the homogeneous austenite of the X120Mn12 steel after reaustenitisation at 900°C. There is a visible recrystallised area of the microstructure due to the PSN mechanism. Etched state

Rys. 3. Mikrostruktura jednorodnego austenitu stali X120Mn12 po reaustenityzacji w 900°C. Widoczny zrekrystalizowany w wyniku mechanizmu PSN obszar mikrostruktury. Stan trawiony

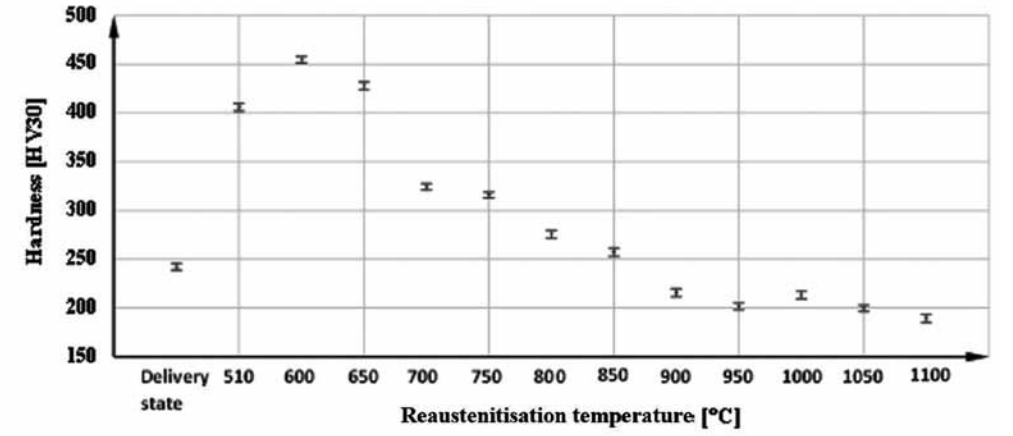

Fig. 4. The change in material hardness values as a function of the reaustenitisation temperature
Rys. 4. Zmiana wartości twardości materiału w funkcji temperatury reaustenityzacji

As a result of the conducted tests, relative changes in wear resistance, when compared to the as-delivery state, were observed. The results are presented in tabular form in **Table 1** and in the graphical representation of the relative percentage change in **Figure 5**. Moreover, the obtained test results were subjected to statistical analysis using the t-Student test for $p < 0.01$ and for $\alpha = 0.05$ (**Fig. 6**). The analysed data were verified for homogeneity of variance and parametricity.

The two-stage heat treatment procedure results in both an increase and a decrease in the wear resistance of X120Mn12 steel, depending on the reaustenitisation temperature.

In the case of the 650°C variant, a statistically significant decrease in the wear resistance of the X120Mn12 steel under abrasion conditions when compared to the as-delivered state was observed – by -6.52% (t-Student test: $p = 0.0027$). This represents the largest decrease in wear resistance in the conducted experiment and is the result of the process of coagulation of $(Fe,Mn)_3C$ carbides and the breakdown of fine-grained pearlite colonies.

In the case of the 750°C variant, a statistically significant increase in the wear resistance of the X120Mn12 steel under abrasion conditions when compared to the as-delivery state was observed – by+6.01% (t-Student test: $p = 0.0033$). This represented the highest increase in wear resistance in the experiment and was achieved for a microstructure with a heterogeneous structure composed of coagulated $(Fe,Mn)_3C$ carbides in an

Table 1. Results of the abrasive wear resistance tests performed according to GOST 23.208-79
Tabela 1. Wyniki badań odporności na zużycie ścierne zrealizowanych według normy GOST 23.208-79

		Heat treatment variants tested for wear resistance												
		Delivery state	510°C | 6h | furnace	600°C	650°C	700°C	750°C	800°C	850°C	900°C	950°C	1000°C	1050°C	1100°C
Mass loss Δm [g]	1	0,0864	0,0880	0,0923	0,0939	0,0826	0,0806	0,0822	0,0846	0,084	0,0876	0,0857	0,0849	0,0865
	2	0,0874	0,0880	0,0915	0,0920	0,0858	0,0825	0,0815	0,0820	0,0863	0,0823	0,0852	0,0816	0,0887
	3	0,0855	0,0849	0,0858	0,0915	0,0813	0,0815	0,0848	0,0836	0,0848	0,0881	0,0852	0,0852	0,0837
	Average	0,0864	0,0870	0,0899	0,0925	0,0832	0,0815	0,0828	0,0834	0,0850	0,0860	0,0854	0,0850	0,0863
Relative wear resistance when compared to the as-delivery state K_b^* [-]			**0,9939**	**0,9618**	**0,9348**	**1,0384**	**1,0601**	**1,0435**	**1,0364**	**1,0165**	**1,0050**	**1,0125**	**1,0163**	**1,0015**

* The relative wear resistance coefficient was calculated according to the GOST 23.208-79 standard (due to the material identity, the coefficient is the ratio of the mass loss of the tested material to the mass loss of the reference material).

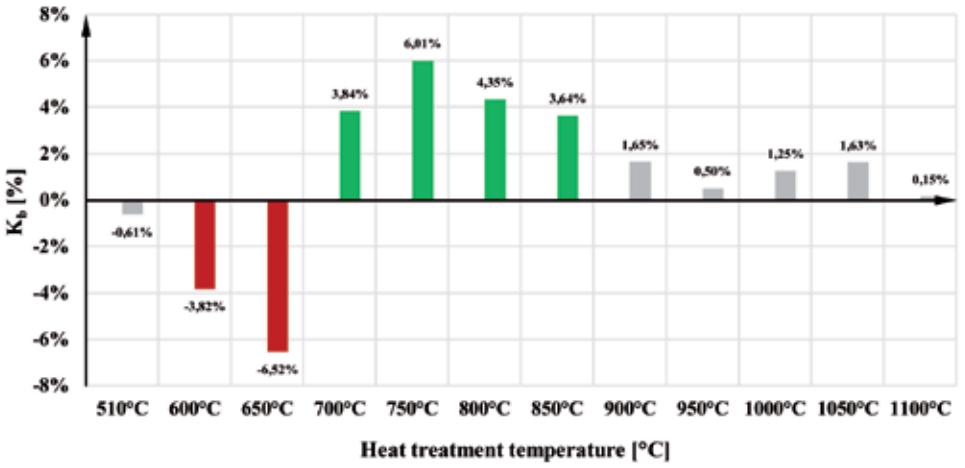

Fig. 5. The relative percentage change in the wear resistance when compared to the delivered state as a function of saturation temperature dependence

Rys. 5. Zależność względnej procentowej zmiany odporności na zużycie ścierne w stosunku do stanu dostarczenia w funkcji temperatury przesycania

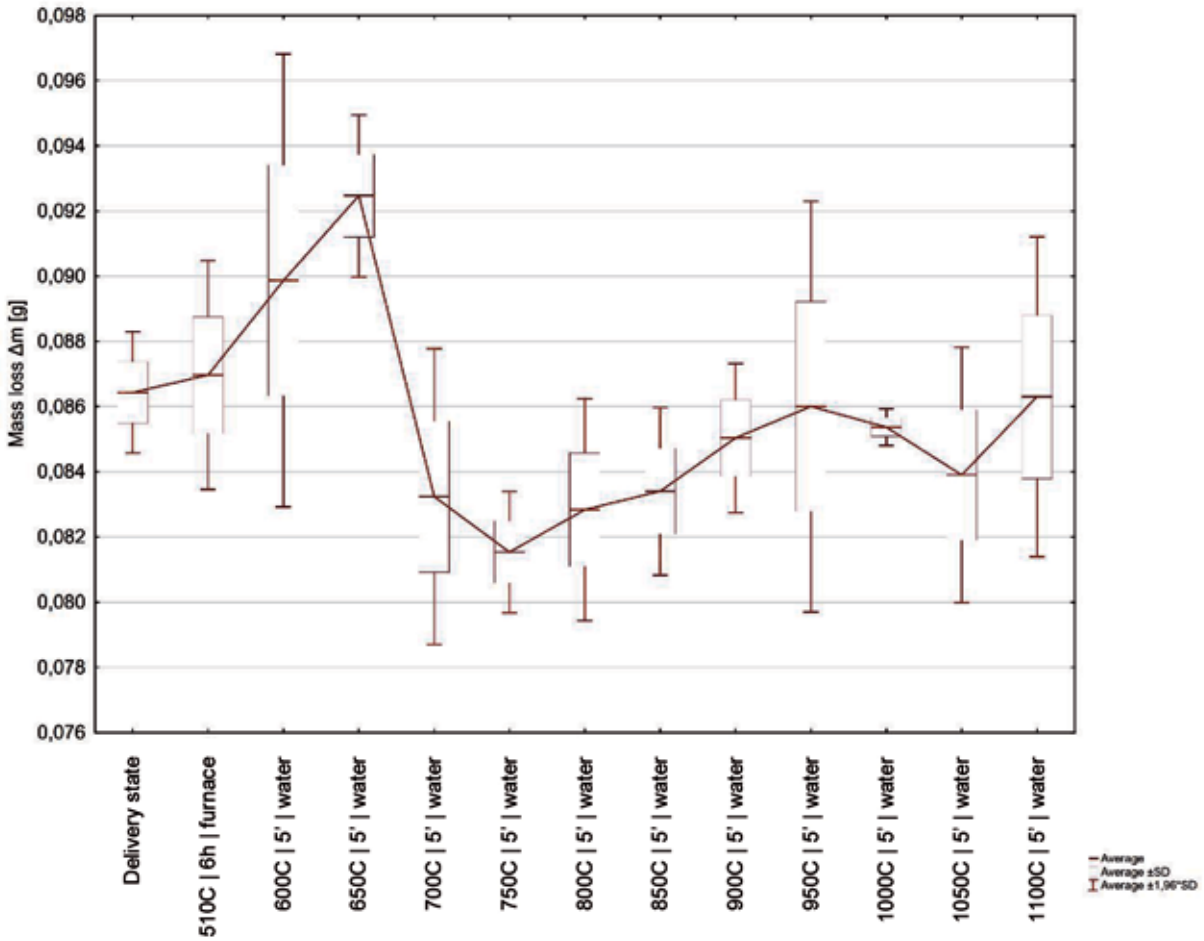

Fig. 6. Box-and-whisker plot showing mass loss after the abrasive wear test for different heat treatment variants of the fine-grained X120Mn12 steel

Rys. 6. Wykres ramka-wąsy obrazujący ubytek masy po teście odporności na zużycie ścierne dla różnych wariantów obróbki cieplnej drobnoziarnistej stali X120Mn12

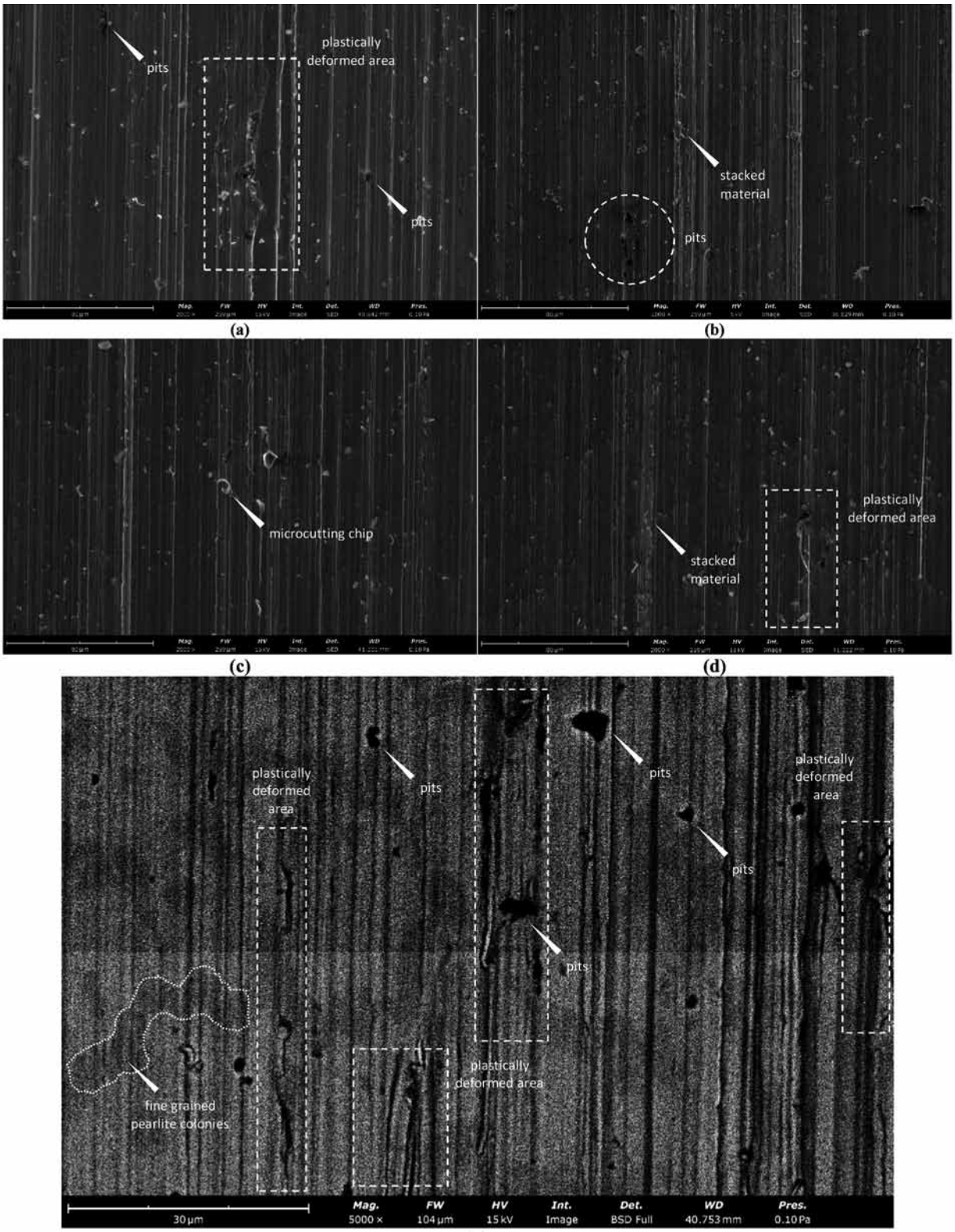

Fig. 7. Morphology of the specimen's surface after the abrasive wear test: (a) delivery condition; (b) after isothermal annealing at 510°C; (c) after reaustenitisation at 750°C; (d) after reaustenitisation at 1000°C – imaged using a SE detector (e). The surface of the sample after isothermal annealing at 510°C (imaged with a BSE detector), partially highlighting the microstructure of the material (location of the fine pearlite colonies)

Rys. 7. Morfologia powierzchni po teście odporności na zużycie ścierne próbki: (a) w stanie dostarczenia; (b) po izotermicznym wygrzewaniu w 510°C; (c) po reaustenityzacji w 750°C; (d) po reaustenityzacji w 1000°C – detektor SE (e). Powierzchnia próbki po izotermicznym wygrzewaniu w 510°C zobrazowana z wykorzystaniem detektora BSE, częściowo uwidaczniającego mikrostrukturę materiału (położenie kolonii drobnopłytkowego perlitu)

austenite matrix. When compared to the 600°C and 650°C variants, the decrease in wear resistance was compensated by the new grains formed by the PSN mechanism, which led to the strengthening of grain boundaries.

In the case of the remaining variants, the significance level was $p > 0.01$, with the gradual decrease in wear resistance in the range of 800°C – 1100°C being related to carbide dissolution and austenite grain growth.

In the case of the state after isothermal annealing, despite a significant increase in material hardness, a slight decrease in wear resistance of -0.61% when compared to the as-delivery state is noticeable. Moreover, the mass losses of individual samples are similar to each other, which results from prolonged isothermal annealing and cooling with the furnace, in turn leading to the homogenisation of the material's microstructure as a result of diffusion processes and it is achieving a state close to phase equilibrium.

The friction processes that occurred during the experiment created conditions for abrasive wear under low pressures, in which hard particles abraded and/or grooved the material surface. Visible longitudinal grooves in the direction of the friction resulting from microcutting and microploughing confirm that the wear mechanism was abrasive. The following figures show sample microscopic images of surfaces after the abrasion resistance test (**Fig. 7**). All the tested samples had the same morphology of grooves and furrows, which were mainly oriented in the direction of the loose abrasive interacting with the sample surface. The material loss during grooving may be due to the exceeding of the critical strain in the material's microvolume or to microfatigue resulting from repeated stacking of the same volume of material. Moreover, strongly plastically deformed areas (**Fig. 7a**, **Fig. 7d**, **Fig. 7e**) and traces of indentations, which result from the removal of larger fragments of the samples (**Fig. 7a**, **Fig. 7b**, **Fig. 7e**), are visible on the sample surface. The observations of the morphology of the sample surface using a BSE detector allowed the distribution of fine-grained pearlite colonies to be visualised (**Fig. 7e**). It was not found that plastically deformed areas, material stacking, and indentations were localised and associated with any microstructure component. Therefore, three dominant abrasive wear mechanisms were identified in the analysed X120Mn12 steel: microploughing, microcutting, and plastic deformation of the material by abrasive particles.

CONCLUSIONS

As a result of the conducted research, it has been found that:

1. A two-stage heat treatment procedure increases and decreases the wear resistance of X120Mn12 steel, depending on the reaustenitisation temperature.
2. The experiment showed that strengthening phenomena caused by the precipitation of globular $(Fe,Mn)_3C$ carbides and the boundaries of new austenite grains resulted in an increase in wear resistance of commercially available fine-grained X120Mn12 steel by approximately 6% when compared to the as-delivery state when reaustenitised at 750°C.
3. An increase in the reaustenitisation temperature translates into a synergy of various mechanisms: carbide coagulation, grain nucleation (PSN), the boundary movement effect, and the final disappearance of $(Fe, Mn)_3C$ carbides, which ultimately affects the increase in austenite grain size. The results of hardness measurements and relative wear resistance reflect the described processes and indicate a decrease in wear resistance in the case of the carbide coagulation process, where the material hardness is relatively high at 454.3 ±3.2 HV30. On the other hand, wear resistance increased due to the synergy of carbide dissolution and new grain formation through the PSN mechanism at a relatively lower hardness of 315.9 ±3.2 HV30.
4. The material hardness decreased with an increase in the reaustenitisation temperature, which is due to the homogenisation of the steel's microstructure through the dissolution of $(Fe, Mn)_3C$ carbides, the disappearance of newly formed grains and the final increase in the austenite grain size.
5. The increase in wear resistance under abrasion conditions does not coincide with the results obtained during tests for coarse-grained steel, resulting from a smaller structure refinement effect due to the PSN mechanism.

REFERENCES

1. Bouaziz O., Allain S., Scott C.P., Cugy P., Barbier D.: High manganese austenitic twinning induced plasticity steels: A review of the microstructure properties relationships. Current Opinion in Solid State and Materials Science 2011, vol. 15, no. 4. Elsevier Ltd, pp. 141–168, doi: 10.1016/j.cossms.2011.04.002.
2. Dastur Y.N., Leslie W.C.: Mechanism of work hardening in hadfield manganese steel. Metallurgical transactions. A, Physical metallurgy and materials science 1981, vol. 12 A, no. 5, pp. 749–759, doi: 10.1007/BF02648339.
3. Dziubek M., Grygier D.: The effect of the wear degree of working elements in a jaw crusher on the operating effectiveness of a two-stage granite grinding system, Tribologia 2021, vol. 295, no. 1, pp. 7–14, Oct., doi: 10.5604/01.3001.0015.4894.
4. Stradomski Z.: Mikrostruktura w zagadnieniach zużycia staliw trudnościeralnych, Częstochowa: Wydawnictwo Politechniki Częstochowskiej, 2010.
5. Fernandes P.E.G., Santos L.A.: Effect of titanium and nitrogen inoculation on the microstructure, mechanical properties and abrasive wear resistance of Hadfield Steels. REM - International Engineering Journal 2020, vol. 73, no. 1, pp. 77–83, doi: 10.1590/0370-44672019730023.
6. Najafabadi V.N., Amini K., Alamdarlo M.B.: Investigating the effect of titanium addition on the wear resistance of Hadfield steel, Metallurgical Research & Technology 2014, vol. 111, no. 6, pp. 375–382, Dec., doi: 10.1051/metal/2014044.
7. Srivastava A.K., Das K.: Microstructure and abrasive wear study of (Ti,W)C-reinforced high-manganese austenitic steel matrix composite. Mater Lett 2008, vol. 62, no. 24, pp. 3947–3950, doi: 10.1016/j.matlet.2008.05.049.
8. Tęcza G., Garbacz-Klempka A.: Microstructure of Cast High-Manganese Steel Containing Titanium. Archives of Foundry Engineering 2016, vol. 16, no. 4, pp. 163–168, doi: 10.1515/afe-2016-0103.
9. Tęcza G., Zapała R.: Changes in impact strength and abrasive wear resistance of cast high manganese steel due to the formation of primary titanium carbides, Archives of Foundry Engineering 2018, vol. 18, no. 1, pp. 119–122, doi: https://doi.org/10.24425/118823.
10. Efstathiou C., Sehitoglu H.: Strengthening Hadfield steel welds by nitrogen alloying, Materials Science and Engineering: A 2009, vol. 506, no. 1–2, pp. 174–179, doi: 10.1016/j.msea.2008.11.057.
11. Tęcza G., Głownia J.: Resistance to Abrasive Wear and Volume Fraction of Carbides in Cast High-manganese Austenitic Steel with Composite Structure. Archives of Foundry Engineering 2015, vol. 15, no. 4, pp. 129–133, doi: 10.1515/afe-2015-0092.
12. Chen C., Lv B., Ma H., Sun D., Zhang F.: Wear behavior and the corresponding work hardening characteristics of Hadfield steel, Tribol Int 2018, vol. 121, pp. 389–399, doi: 10.1016/j.triboint.2018.01.044.
13. Jafarian H.R., Sabzi M., Mousavi Anijdan S.H., Eivani A.R., Park N.: The influence of austenitization temperature on microstructural developments, mechanical properties, fracture mode and wear mechanism of Hadfield high manganese steel, Journal of Materials Research and Technology 2021, vol. 10, pp. 819–831, doi: 10.1016/j.jmrt.2020.12.003.
14. Mousavi Anijdan S.H., Sabzi M.: The Effect of Heat Treatment Process Parameters on Mechanical Properties, Precipitation, Fatigue Life, and Fracture Mode of an Austenitic Mn Hadfield Steel, J Mater Eng Perform 2018, vol. 27, no. 10, pp. 5246–5253, doi: 10.1007/s11665-018-3625-y.
15. Azadi M., Pazuki A.M., Olya M.J.: The Effect of New Double Solution Heat Treatment on the High Manganese Hadfield Steel Properties. Metallography, Microstructure, and Analysis 2018, vol. 7, no. 5, pp. 618–626, doi: 10.1007/S13632-018-0471-0.
16. Bandanadjaja B., Hidayat E.: The effect of two-step solution heat treatment on the impact properties of Hadfield austenitic manganese steel. J Phys Conf Ser 2020, vol. 1450, no. 1, p. 012125, doi: 10.1088/1742-6596/1450/1/012125.
17. Mishra S., Dalai R.: A comparative study on the different heat-treatment techniques applied to high manganese steel, Mater Today Proc 2021, vol. 44, pp. 2517–2520, doi: 10.1016/j.matpr.2020.12.602.

18. Ayadi S., Hadji A.: Effect of Chemical Composition and Heat Treatments on the Microstructure and Wear Behavior of Manganese Steel. International Journal of Metalcasting 2021, vol. 15, no. 2, pp. 510––519, doi: 10.1007/s40962-020-00479-2.
19. Rollett A., Humphreys F., Rohrer G.S., Hatherly M.: Recrystallization and Related Annealing Phenomena: Second Edition, pp. 1–628, 2004, doi: 10.1016/B978-0-08-044164-1.X5000-2.
20. Lashgari H.R., Zangeneh S.: Particle-Stimulated Nucleation (PSN) in the Co–28Cr–5Mo–0.3C Alloy, Metals 2020, Vol. 10, Page 671, vol. 10, no. 5, p. 671, doi: 10.3390/MET10050671.
21. Sidor J., Petrov R.H., Kestens L.: Texture Control in Aluminum Sheets by Conventional and Asymmetric Rolling, Comprehensive Materials Processing 2014, vol. 3, pp. 447–498, doi: 10.1016/B978-0-08-096532-1.00324-1.
22. Porter J.R., Humphreys F.J.: Nucleation of recrystallization recrystallisation at second-phase particles in deformed copper alloys. http://dx.doi.org/10.1179/msc.1979.13.2.83, vol. 13, no. 2, pp. 83–88, Feb. 2013, doi: 10.1179/MSC.1979.13.2.83.
23. zum Gahr K.-H., Eldis G.T.: Abrasive wear of white cast irons, Wear 1980, vol. 64, no. 1, pp. 175–194, doi: 10.1016/0043-1648(80)90101-5.
24. Hurricks P.L.: Some metallurgical factors controlling the adhesive and abrasive wear resistance of steels. A review, Wear 1973, vol. 26, no. 3, pp. 285–304, doi: 10.1016/0043-1648(73)90184-1.
25. Modi O.P., Prasad B.K., Jha A.K., Dasgupta R., Yegneswaran A.H.: Low-Stress Abrasive Wear Behaviour of a 0.2% C Steel: Influence of Microstructure and Test Parameters, Tribol Lett 2003, vol. 15, no. 3, pp. 249–255, doi: 10.1023/A:1024865220280.
26. Fulcher J.K., Kosel T.H., Fiore N.F.: The effect of carbide volume fraction on the low stress abrasion resistance of high Cr-Mo white cast irons, Wear 1983, vol. 84, no. 3, pp. 313–325, doi: 10.1016/0043-1648(83)90272-7.
27. Doğan Ö.N., Hawk J.A.: Effect of carbide orientation on abrasion of high Cr white cast iron, Wear 1995, vol. 189, no. 1–2, pp. 136–142, doi: 10.1016/0043-1648(95)06682-9.
28. Mutton P.J., Watson J.D.: Some effects of microstructure on the abrasion resistance of metals, Wear 1978, vol. 48, no. 2, pp. 385–398, doi: 10.1016/0043-1648(78)90234-X.
29. Gahr Z.: Microstructure and Wear of Materials 1st Edition. Elsevier Science Ltd 1987, vol. 37, no. 412, p. 16.
30. Gates J.D.: Two-body and three-body abrasion: A critical discussion, Wear 1998, vol. 214, no. 1, pp. 139––146, Jan., doi: 10.1016/S0043-1648(97)00188-9.
31. Machado P.C., Pereira J.I., Sinatora A.: Abrasion wear of austenitic manganese steels via jaw crusher test, Wear 2021, vol. 476, Jul., doi: 10.1016/j.wear.2021.203726.
32. Dziubek M., Rutkowska-Gorczyca M., Dudziński W., Grygier D.: Investigation into Changes of Microstructure and Abrasive Wear Resistance Occurring in High Manganese Steel X120Mn12 during Isothermal Annealing and Re-Austenitisation Process, Materials 2022, vol. 15, no. 7, p. 2622, doi: 10.3390/ma15072622.